# 7 Hadron Physics and non-perturbative QCD

## 7.1 Introduction

There is overwhelming theoretical and experimental evidence that QCD is the theory of strong interactions. Yet, QCD is to a large extent unsolved. In particular, standard perturbation theory becomes completely unreliable in the infrared regime, where QCD is strongly coupled. Experimentally, there is a large number of facts that lack a detailed qualitative and quantitative explanation.

The most spectacular manifestation of our lack of theoretical understanding of QCD is the failure to observe the elementary degrees of freedom, quarks and gluons, as free asymptotic states (color confinement) and the occurrence, instead, of families of massive mesons and baryons (hadrons) that form approximately linear Regge trajectories in the mass squared. The internal, partonic structure of hadrons, and nucleons in particular, is still largely mysterious. Since protons and neutrons form almost all the visible matter of the Universe, it is of basic importance to explore their static and dynamical properties in terms of quarks and gluons interacting according to QCD dynamics. All issues discussed in this Chapter share this common motivation.

Several theoretical models have been developed through the years to describe the hadronic interactions starting from very basic principles. QCD has a remarkable success in describing the high energy and large momentum transfer processes, where the quarks in the hadrons behave, to some extent, as free particles and a perturbative approach can therefore be used. In this simple approach a fast moving nucleon is essentially considered as a collection of free partons, all moving parallel to the parent nucleon (collinear configuration). Nevertheless, the largest fraction of hadronic interactions involve low momentum transfer processes in which the effective strong coupling constant is large and a description with a perturbative approach is not adequate. Even at large momentum transfer, the simple collinear picture is not supported by experiments and fails badly in explaining many spin-dependent effects.

In most interactions involving hadrons, the dynamical properties and degrees of freedom of quarks and gluons combine with some non-perturbative QCD aspects, to give measured physical quantities. The description of the attempts to understand such processes is the purpose of the “Hadron physics and non-perturbative QCD" Chapter, which is then structured into several main issues, according to the following scheme.

In Section **7.2** a concise description of the theoretical framework underlying the non-perturbative approach to QCD is presented. Some of the issues are mentioned for consistency, although they will not be further discussed in the following Sections.

In Section **7.3** the most recent progress on the study, both theoretical and experimental, of the nucleon partonic structure is presented. Particular emphasis is given to the 3-dimensional structure, both in momentum and coordinate space: it represents a new phase in our image of the nucleon, which goes beyond the traditional and simple 1-dimensional picture of a fast moving nucleon as a bunch of collinearly moving partons.

Section **7.4** reports on hadron spectroscopy, which looks at the total quantum numbers of bound states of quarks and gluons. It shows that more and more precise experimental data are not yet well understood, while more unconventional, although possible, bound states are still not observed.

Section **7.5** deals with the study of the proton–proton total and elastic cross sections, and of the diffractive dissociation processes; these are of fundamental importance to understand the mechanisms of hadronic interactions and their evolution with respect to the center of mass energy and momentum transfer. The dynamical QCD properties of partons become crucial when processes involving hadrons at large energies take place and the role of multi parton interactions, rather than a single elementary interaction, has to be explored and understood. The latter issue is discussed in Section **7.6**.

A precise knowledge of the cross sections and of the properties of particle production in hadronic collisions is crucial in order to reduce the systematic errors in several measurements of great astrophysical interest. This issue is discussed in Section **7.7**.

For each of the above topics the prospects for new measurements at existing and future experimental facilities are considered and discussed. Emphasis is given to the phenomenological aspects of QCD and its application, to the understanding of the hadronic structure and its non-perturbative features and to the related experiments. An executive summary is given in Section **7.8**.

### 7.2 Confinement and non-perturbative QCD

The first challenge for any theoretical understanding of QCD is to describe the mechanism underlying color confinement and to reproduce qualitatively and quantitatively the spectrum of mesons and baryons, as opposed to the spectrum of quarks and of massless gluons that occur in perturbation theory. One would also like to take properly into account non-perturbative contributions to various Standard Model amplitudes and to predict the properties of strong interactions in extreme conditions, such as high temperature and density, i.e. to map the QCD phase diagram.

In absence of a systematic perturbative approach, a theoretical tool based on first principles is provided by lattice QCD simulations [735]. The theory, in its path integral formulation, is discretised on a space-time lattice and then computed numerically via Monte-Carlo algorithms. Nowadays, thanks to technological and theoretical advancements, lattice QCD is a mature field, which, however, requires a continuous effort to sustain the computational requirements and the algorithmic developments.

Another promising theoretical tool is large-$N$ QCD [736], that allows us to describe QCD as a theory of an infinite number of mesons and glueballs weakly-coupled at all energy scales, as opposed to quarks and gluons that occur in perturbation theory.

Both large-$N$ and lattice QCD predict the existence of glueballs, experimentally not clearly identified yet. Spectral properties are particularly accessible to lattice simulations: the accuracy for glueball and meson masses in QCD with physical quark masses [737] or in large-$N$ computations [738–740] are not presently satisfactory yet, but it is conceivable that the accuracy will improve over the next 10 years. The systematic search for glueballs, and more generally of mesons and baryons, is one of the experimental challenges in the near future, in the reach of dedicated experiments such as BESIII (Beijing) and JLab (Newport News). Other experimental facilities able to explore the glueball and hadron spectrum are COMPASS, J-PARC (Japan), LHCb (CERN), and FAIR (Darmstadt) (to start in 2018).

On the theoretical side, recent developments go in the direction of the computation of the large-$N$ QCD $S$-matrix [741], which is likely to remain inaccessible to Lattice QCD except for some interesting special cases [742]. This opens the way to a direct comparison with data provided by past (BaBar) and future experiments, such as FAIR (Darmstadt 2018) and JLab about meson form factors.

Moreover, glueball production, together with other interesting non-perturbative aspects of QCD are in the experimental reach of diffractive phenomenology, like high-energy $p$-$p$ exclusive forward scattering, that allows to get a very accurate measure of the much smaller energy and momentum of the resonances produced in the central region (see Section 7.5.3). It is indubitable that this is a field where high precision experimental measurements can meet theoretical predictions from the lattice or from large-$N$ QCD and possibly lead to a better understanding of strong interactions.

Another interesting experimental direction is the exploration of the QCD phase diagram by heavy-ion collision experiments, in particular regarding the detection of the transition to a Quark-Gluon Plasma phase, that may allow a comparison with lattice measurements. One should stress the investigation of collective and transport properties of the strongly coupled medium produced in such collisions, the search for a possible critical endpoint in the phase diagram at high baryon density and the possible rich phenomenology of strong interactions in the presence of strong magnetic fields [743], which are expected in the early stages of non-central heavy ion collisions. All that is relevant to many experiments at LHC (ALICE, ATLAS, CMS), at RHIC and FAIR. Lattice simulations are already providing precision results regarding QCD thermodynamics with and without external background fields, while new algorithms are needed to properly deal with the complex nature of the path integral measure in the presence of a finite

baryon density. The achievement of accurate results on transport properties is less trivial, since lattice simulations deal intrinsically with equilibrium physics.

There is one final issue, somehow at the intersection between the understanding of QCD and the search for new physics, that involves the computation of the QCD corrections to the muon anomalous magnetic moment, that is likely to be affected both by theoretical developments in computation of light-by-light scattering [741, 744] and by direct experimental measures of the relevant form factors [744].

### 7.3 The nucleon structure

From the perspective of hadron physics the main new recent interest in the nucleon structure is focused on its 3-dimensional partonic configuration, describing the spatial distribution and the intrinsic motion of quarks and gluons inside protons and neutrons. However, the usual integrated partonic distributions, depending only on the longitudinal momentum fraction of the parent nucleon carried by the parton, play a crucial role in many high energy processes and still have large uncertainties which affect the theoretical calculations. A short assessment of the actual situation is given as a starting point.

#### *7.3.1 Parton distribution functions*

Parton distribution functions, henceforth referred to as PDFs, are an essential ingredient of any computation of cross sections at hadron colliders, based on QCD [745]. According to the collinear factorisation of the cross section into short- and long-distance components, delimited by a factorization scale $\mu_F$, the cross section for the production of a final state $X$ in the hard scattering initiated by two hadrons $h$ and $h'$, with four-momenta $P$ and $P'$ and squared center-of-mass energy $s = (P + P')^2$, can be expressed as the convolution of PDFs and parton cross sections:

$$\sigma_{hh' \to X} = \sum_{i,j} \int_0^1 \mathrm{d}x_1 \, \mathrm{d}x_2 \, f_i^h(x_1, \mu_F^2) \, f_j^{h'}(x_2, \mu_F^2) \times \hat{\sigma}_{ij \to X}(x_1, x_2, s, \alpha_s(\mu_R^2)) \tag{50}$$

where $f_i^h$ are the PDFs for the hadron $h$, the indices $i$, $j$ run over all parton types, $\hat{\sigma}_{ij \to X}$ is the parton cross section for incoming partons with momenta $p_1 = x_1 P$ and $p_2 = x_2 P'$, and $\alpha_s(\mu_R^2)$ is the strong-coupling constant evaluated at the renormalisation scale $\mu_R$.

Once the functional form of a PDF at a given starting scale $Q_0^2$ is fixed, its evolution at any given scale $Q^2 > Q_0^2$ can be described in perturbative QCD with the Dokshitzer, Gribov, Lipatov, Altarelli and Parisi (DGLAP) equations [746–748]. The PDF at the starting scale $Q_0^2$ needs to be determined from fits to experimental data. In the current determination of PDFs from the global QCD analysis of experimental data [749–753], measurements of deep inelastic scattering (DIS, $\ell N \to \ell X$) at lepton-nucleon colliders provide crucial information. Additional constraints are provided by fixed target experiments, neutrino data, and data from proton-antiproton and proton-proton collisions.

A precise knowledge of the PDFs is a fundamental prerequisite for the physics program at hadron colliders, including the measurement of cross sections, the determination of the fundamental parameters of the SM, and the search for physics beyond the SM. In Run II of the LHC collider, several fundamental measurements, including Higgs boson production via gluon-fusion processes, the measurement of the mass of the $W$ boson, and the extraction of the weak-mixing angle from the $Z$ boson forward-backward asymmetry, are likely to be dominated by the PDFs uncertainty, as discussed in Section 4.2.1 and Appendix A.1. Therefore, it is of fundamental importance to invest effort on both experimental and theoretical aspects of the PDFs determination.

Moderate discrepancies, at the level of one to two standard deviations, are observed in the comparison of predicted cross sections for the production of Higgs bosons at the LHC, based on different PDF sets [754, 755]. Since the origin of such differences in the Higgs prediction between the various PDF sets is not yet understood, it should be considered as an additional PDF uncertainty, according to the

PDF4LHC convention [756]. The total PDF uncertainty on gluon-fusion Higgs production cross section in proton-proton collisions at a center-of-mass energy of $8$ TeV and $14$ TeV is estimated at the level of $5\%$; if such a PDF uncertainty is not reduced, it will be one of the limiting factors in the accuracy for the determination of the Higgs boson couplings from the LHC data.

The QCD analysis of the full LHC data set collected in Run I, and of the future Run II measurements, will provide further constraints on the extraction of the PDFs, and significant reduction of the PDF uncertainties. However, a much improved determination of the PDFs can be achieved by measurements of DIS in $e\,p$ collisions at higher energies and higher luminosities, as those achievable by the LHeC collider [97].

### *7.3.2 The 3-dimensional picture of the nucleon: theory*

For sufficiently inclusive processes, at leading order, the PDFs describe a fast-moving hadron as a collection of fast-moving collinear partons, each one sharing a fraction $x$ of the parent hadron momentum. Many past experiments on DIS of lepton beams off nucleons exposed how partons share this momentum [749–753]. However, this one-dimensional view provides only limited information on the nucleon structure. For example, it does not answer the question of how partons share the nucleon's spin. Worldwide experimental measurements in the last two decades have shown that the spin of quarks and antiquarks contribute about 30% to the nucleon spin, and that the total spin carried by the gluons is non-zero but not sufficient to account for the missing 70% [757]. Therefore, the orbital angular momentum (OAM) of partons needs also to be addressed; understanding (and estimating) this contribution requires a description of the nucleon structure that goes beyond a simple one-dimensional view [758–760].

The most direct generalisation of PDFs is a new class of objects denoted as Transverse Momentum Dependent PDFs (TMD PDFs; for brevity, TMDs), that describe the joint distributions in $x$ and in the parton transverse momentum $\boldsymbol{k}_\perp$ (transverse with respect to the parent nucleon's momentum) [761–765]. A similar generalisation holds for the fragmentation functions (TMD FFs). The TMDs are encoded in the cross section for semi-inclusive DIS (SIDIS, $\ell\,N \to \ell\,h\,X$) [765]. SIDIS has two natural scales: the lepton large momentum transfer, $Q$, and the transverse momentum, $P_T$, of the final hadron. If $P_T \ll Q$, a suitable factorisation theorem allows to isolate TMDs in the SIDIS cross section [766–768], which can be expressed as a convolutions of TMDs and perturbative elementary interactions: thus, measuring the $\boldsymbol{P}_T$ distribution reveals details of the transverse motion of the initial parton inside the target.

At leading twist, eight independent TMDs can be defined, each one appearing in a specific SIDIS (spin) asymmetry with its own peculiar dependence on the nucleon transverse spin and final hadron angles [765]. Three of them survive after integrating upon the parton $\boldsymbol{k}_\perp$, recovering the three collinear PDFs that are needed to describe the spin structure of a fast-moving nucleon in the collinear framework: the unpolarised, the helicity, and the transverse polarisation (transversity) distributions. The transversity distribution is the least known of the three, although it has been shown to be different from zero in a series of SIDIS measurements by HERMES [769] and COMPASS [770–772]. It is related to the tensor charge of the nucleon and its difference from the helicity distribution quantifies the relativistic effects in the hadronic structure. Among the other five TMDs, two of them have received particular attention since they depend on fundamental properties of QCD such as its color gauge invariance. For example, the so-called Sivers function [773] describes how the $\boldsymbol{k}_\perp$ distribution of an unpolarised quark is distorted by the transverse polarisation, $\boldsymbol{S}_T$, of its parent nucleon. As a consequence, in a SIDIS process off a transversely polarised nucleon, the $\boldsymbol{P}_T$ distribution of the final detected hadron is asymmetric with respect to flipping $\boldsymbol{S}_T$. The Sivers effect is thought to arise due to the residual color interactions between the struck parton and the target remnants [774–776]. It can happen also in Drell-Yan processes with a transversely polarised nucleon. In this case, however, the color gauge invariance is realised through initial state interactions between the nucleon's annihilating quark and the remnants of the other colliding hadron [777]. The net result is that the Sivers effect would have an opposite sign in Drell-Yan with respect to SIDIS [778,779]. This process dependence (or non-universality) of the Sivers function is a fun-

damental prediction based on the color gauge invariance of QCD. Therefore, an experimental verification of this sign change is of crucial importance in hadronic spin physics and is currently under investigation by the COMPASS collaboration, using for the first time a high energy beam of pions scattering off a transversely polarised fixed nucleon target [780].

Experimental evidence of the Sivers effect in SIDIS, and of different "QCD spin-orbit" effects involving other TMDs, will be described in the next subsection, together with an account of running and planned dedicated future experiments.

In this new scenario, multi-dimensional imaging of hadrons can be alternatively approached through hard exclusive processes like Deeply-Virtual Compton Scattering (DVCS, $\ell N \to \ell N \gamma$) [781]. For a lepton momentum transfer $Q^2$ much larger than the squared change in the nucleon target momentum [$Q^2 \gg -t = -(P - P')^2$], the so called Generalised Parton Distributions (GPDs) can be factorised in the cross section [781, 782]. They depend on $t$, $x$, and on the change $\xi$ in the longitudinal parton momentum. For $\xi = 0$, the two-dimensional Fourier transform of the $t$ dependence converts the GPDs into a spatial distribution of partons in the transverse plane at a given $x$ [783, 784]. This may be regarded as a tomography of the nucleon, where two-dimensional spatial images are taken for different "slices" of the parton momentum $x$. Thus, the GPDs encompass in a unique framework the information on spatial densities (form factors) and on longitudinal momentum densities (PDFs).

For DVCS on a transversely polarised nucleon, the nucleon helicity-flip GPD $E$ describes a distorted spatial distribution. It is the analogue in position space of the Sivers effect [785]. Indeed, a dynamical connection between the two phenomena can be formulated, although in a model dependent way since it is based on the non-perturbative description of color interactions between struck and spectator partons [786]. The GPD $E$ is linked to the problem of calculating the parton OAM [787]. In fact, both the GPD $E$ and its nucleon helicity-non-flipping partner $H$ enter the so-called Ji's sum rule [788], where in the forward limit ($\xi = 0, t = 0$) the sum of their second Mellin moments gives the total angular momentum carried by partons. However, separating for each flavour the orbital contribution from the helicity is still a matter of debate, because it involves several conceptual aspects at the core of non-abelian gauge theories (for a recent review, see Ref. [789] and references therein).

A direct experimental access to the whole kinematic dependence of GPDs is not possible: the $x$ dependence is integrated over in the scattering amplitude. To unravel GPDs requires dedicated, long-term measurements of a variety of observables like cross sections, beam and target spin asymmetries for both longitudinally and transversely polarised targets, as well as using different channels [790, 791]. Factorisation theorems for GPDs exist not only for DVCS but also, *e.g.*, for Deeply-Virtual Meson Production (DVMP, $\ell N \to \ell N M$) [792]. While DVCS or DVMP for neutral vector mesons involve GPDs of gluons or of sea quarks in particular flavour combinations [793], the DVMP for pseudoscalar mesons provides access to different flavour combinations of GPDs for longitudinally polarised quarks and anti-quarks [794].

We remark that TMDs and GPDs give independent and complementary information on the dynamics of partons confined inside hadrons. In fact, the spatial distributions obtained from GPDs are not correlated to the momentum distributions from TMDs [764]. While from GPDs we get "spatial" tomographies of the nucleon, from TMDs we can get independent "momentum" tomographies. Combining the two pictures will represent a new landmark in the process of understanding QCD confinement.

### *7.3.3 The 3-dimensional picture of the nucleon: experiments*

As described in the previous subsections Deep Inelastic Scattering experiments provide the standard tool to investigate the structure of the nucleon. More recently, the importance of semi-inclusive DIS (SIDIS) experiments, that is DIS experiments in which at least one hadron from the current jet is detected, has increased considerably, in particular to obtain information on the new Transverse Momentum Dependent partonic distributions (TMD PDFs). In SIDIS the investigations of TMDs cannot be decoupled from the

measurements of the fragmentation functions, which also may depend on the transverse motion of the final hadron with respect to the fragmenting parton (TMD FFs). Then, complementary information must be gathered from $e^+e^-$ and $p\,p$ colliders.

DIS and SIDIS experiments are being performed at CERN (COMPASS) and at JLab (CLAS); $e^+e^-$ data have been collected at SLAC (BaBar) and KEK (Belle), while polarised $p\,p$ processes are studied at BNL (RHIC). Several important conclusions may be drawn from a huge amount of activities over the past 20 years:

- The decomposition of the spin of the nucleon in terms of its constituent partons is a highly non-trivial theoretical problem, still unsettled to-day
- The spin of the constituent partons cannot account for the whole nucleon spin; there must be a sizeable contribution from the orbital angular momentum (OAM) of the partons, still unmeasured and still incalculable.
- The standard (collinear) QCD description of a nucleon in terms of two PDFs, $f_1(x)$ and $g_1(x)$, has to be complemented by a third function, the so-called transversity distributions, $h_1(x)$ [795]. The measurements of HERMES and COMPASSS [769–772] have shown that $h_1$ is different from zero. First extractions of transversity from SIDIS and $e^+e^-$ data have already been performed [796–801].
- The discovery of $h_1$ is not the only consequence of a renewed attention to transverse spin effects: the description of the nucleon in terms of 1-D PDFs has been generalised to include two more dimensions, defined either by the parton intrinsic momentum $\boldsymbol{k}_\perp$ (in momentum space) or by the impact parameter $\boldsymbol{b}_T$ (in coordinate space). In the first case one talks of TMDs, in the second of Generalized Parton Distributions (GPDs).
- The TMDs and the GPDs give a 3-D image of the nucleon which is much more detailed than the 1-D image given by the three collinear PDFs. Most important, they provide tools to access the missing contribution to the nucleon spin, namely the parton OAMs.

As described above, to access information on the TMDs one needs to perform SIDIS experiments; a complete 3-D description of the nucleon requires, at leading-twist, the knowledge of 8 TMD PDFs. So far the most important results have been obtained by the HERMES and COMPASS Collaborations by scattering high energy leptons off transversely polarised nucleons; such results regard essentially the Sivers function which has definitely been shown to be different from zero [802–804]. This TMD is particularly important because it quantifies a correlation between the intrinsic quark momentum and the spin of a transversely polarised nucleon and, due to parity invariance, must be related to the parton orbital angular momentum. The $\boldsymbol{P}_T$ dependence of the final hadron, as measured in the unpolarised cross sections or multiplicities [805, 806], has given information on the unpolarised TMD and demands the presence of the quark intrinsic motion, with a $\boldsymbol{k}_\perp$ dependence which seems to be well described by Gaussian distributions [807].

So far, some knowledge has been obtained on the unpolarised distribution $f_1(x, \boldsymbol{k}_\perp)$, the helicity distribution $g_1(x, \boldsymbol{k}_\perp)$, the transversity distribution $h_1(x, \boldsymbol{k}_\perp)$ and the Sivers distribution $f_1^\perp(x, \boldsymbol{k}_\perp)$, while the other four are essentially unknown. In particular very little is known on the so-called Boer-Mulders TMD, which gives the interesting correlation between the quark's transverse motion and its spin, which, again, must involve the quark orbital angular momentum. A non-vanishing Boer-Mulders function would allow subtle spin effects even in processes involving unpolarised protons, which seems to be the case with the azimuthal dependence measured in Drell-Yan processes.

In the TMD sector basically all the existing information has come from the HERMES and COMPASS Collaborations, but HERMES has now stopped operating and in the near future of COMPASS only SIDIS measurements on a liquid hydrogen target [780] are foreseen, in the years 2016 and 2017, which hopefully will provide information on the Boer-Mulders function. On the contrary, JLab experiments at the upgraded energy of 12 GeV (JLab 12) should provide a wealth of SIDIS data on transversely

polarised targets, albeit at lower energy, *i.e.* mainly at large $x$ values [808].

It should be added that the investigation of transverse spin effects and the introduction of TMDs has finally allowed an understanding of the huge and mysterious single spin effects known for decades and measured in proton-proton interactions over a very large energy range [809].

Turning to the 3-D picture of the nucleon in coordinate space, as stated above, the GPDs encode such information. The GPDs can be extracted from measurements of exclusive reactions, like deeply virtual Compton scattering (DVCS) or deeply virtual meson production (DVMP), in which a high energy lepton scatters off a nucleon and the final state consists of only the scattered lepton, the nucleon and a photon or a produced meson. The extraction of GPDs from experimental results needs a large amount of data on hard exclusive processes over a broad kinematic range. So far information in the high energy regime at low $x$ was provided by H1 [810, 811] and ZEUS [812] at DESY and, in the low energy regime at high $x$ by HERMES [813] and JLab [814]. The COMPASS measurements will provide a connection between these measurements by covering the kinematic regime of $x \simeq 0.1$, where both sea and valence quarks are equally important. Some DVMP measurements have already been performed by COMPASS [815] on a transversely polarised proton target, in parallel to the transverse single spin effects in SIDIS, and future measurements of DVCS and DVMP on a liquid hydrogen target [780] are already planned for the years 2016 and 2017. On a longer time scale, measurements of DVCS on a transversely polarised proton target are also planned, to access the GPD $E$ and possibly exploit Ji's sum rule to get the total angular momentum of a quark inside a polarised nucleon. Very much as for the SIDIS measurement, JLab 12 will be a major player in this field in the next decade, in the complementary large $x$-value range.

On the horizon, the best facility to pursue the investigation of the spin structure of the nucleon is a polarised electron–polarised proton (or ion) collider (EIC). An international study group has been working for at least 10 years on two parallel projects [816]; one to be realised at Brookhaven National Laboratory (BNL), which would exploit the existing high energy (up to 250 GeV) polarised proton beam of RHIC, adding an electron machine, and one to be realised at JLab, which would exploit the 12 GeV polarised electron beam, adding a polarised proton machine. Both proposals are attractive, in both cases there are several options with different values of the center of mass energy ($\sqrt{s}$ = 45–175 GeV for BNL, 12–140 GeV for JLab), and most likely the decision of which one (if any) to choose will be a political one. The scientific programme is impressive and one indeed expects that a 3-D imaging of the nucleon could be achieved. The spin program will not be the only goal of the project: the exploration of the gluon content of the nucleon, the assessment of the conditions which lead to the saturation of the gluon density and the modifications induced by the nuclear environment are also very important goals. A European team has tried to see whether a polarized electron-proton collider could be built at FAIR [817], possibly using for the proton ring the antiproton storage ring HESR foreseen for the PANDA experiment, but the chances of such a project being pushed forward are probably very small. Most recently, a proposal for a similar EIC project in China has been presented [818], which seems to have reached some level of approval and clearly deserves full attention.

From a different perspective, one finds another project of interest for the QCD structure of the nucleon, namely a Large Hadron Electron Collider at CERN (LHeC@CERN) [97]. The project sits at the high energy frontier ($\sqrt{s}$ = 800–1300 GeV), and utilises a high energy proton beam from LHC, colliding with a newly built electron beam of 60 GeV (or possibly 140 GeV). The physics programme complements the LHC and its discovery potential for physics beyond the Standard Model with high precision deep inelastic scattering measurements. The LHeC would continue the path of deep inelastic scattering (DIS) into unknown areas of physics and kinematics. With a design luminosity of $10^{33}$ cm$^{-2}$ s$^{-1}$ the LHeC is projected to exceed the integrated HERA luminosity by two orders of magnitude, which means that the parton distributions can be determined with unprecedented accuracy. No polarisation of the proton beam is envisaged, thus the issues of the QCD spin structure of the nucleon cannot be addressed by this machine, whose scopes are clearly different.

## 7.4 Hadron spectroscopy

Until the end of the previous century, all known hadrons could be described by Quantum Chromodynamics (QCD) as bound states of either a quark and an antiquark (integer spin particles known as "mesons"), or three quarks (half integer spin objects called baryons). In principle, QCD can predict the existence of a larger variety of hadrons, made of two quarks and two antiquarks (tetraquarks or meson molecules), or four quarks and an antiquark (pentaquarks), six quarks (exaquarks), or even no quarks (glueballs). For more than forty years such exotic states have been searched for without success. A notable exception is represented by the long-standing problem of identification of the light scalar mesons, which are hardly explainable as simple $q\bar{q}$ systems, but are more successfully accommodated to form a nonet with inverted mass hierarchy, as suggested in references [819], using the tetraquark model. With the advent of B-factories [820], together with the discovery of many missing pieces of the standard spectra, a plethora of 'exotic' candidates have been claimed by the experiments. Heavy-light diquark-antidiquark mesons have been proposed for the first time in [821] where, together with the interpretation of the X(3872) as a compact tetraquark meson, a complete scheme for the description of similar expected states was proposed. The picture was updated in [822] in view of the most recent experimental findings.

This review will first focus on the relatively simple pattern describing all heavy-light pseudoscalar and vector mesons, and the heavy baryons, whose spectroscopy have benefited not just from B-factories, but also from the Tevatron and LHC in the recent past. Then we will review the recent progress in heavy quarkonium spectroscopy [823], which has experienced a second renaissance [824] in the last decade, with the unexpected discoveries of states above or across open flavour thresholds, which have opened new pathways to the missing narrow states, solving old puzzles, but raising intriguing new questions.

### *7.4.1 Heavy Mesons and Baryons*

In spite of the recent achievements of lattice QCD (summarised in Fig.95) we are still lacking a full understanding of the spectroscopy of light hadrons starting from the QCD Lagrangian [825]. Only 1.2 percent of the nucleon mass (and therefore of the visible mass of the Universe) is due to the Higgs coupling: the hadron masses are mostly due to the dynamics of the strong force.

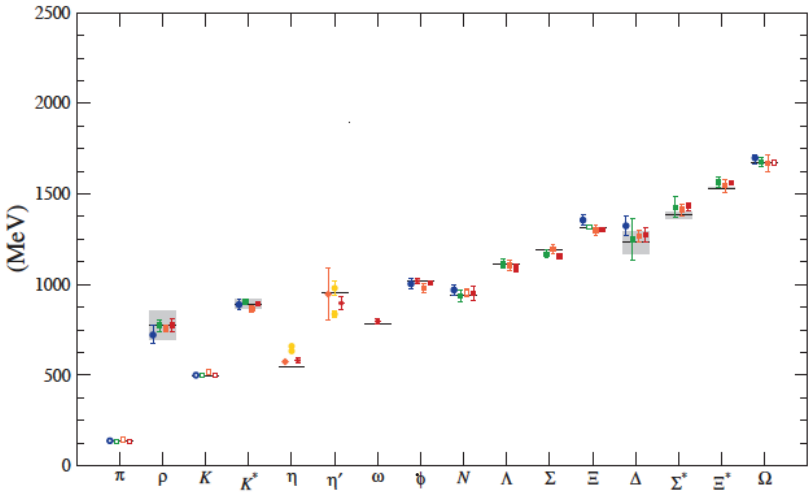


**Fig. 95:** Summary of most recent lattice results on u,d,s mesons and baryons, from Ref. [826]

The bare masses of the $u$ and $d$ quarks are approximately 3 and 5 MeV, and all the rest comes from the gluonic field which binds together the three quarks in the nucleon, in relativistic motion around the common center of mass. It must be noticed that the mass difference between the down and up quarks

has a crucial role in determining the mass difference between the neutron and the proton: if only QED effects were present, protons would decay to neutrons.

In order to decouple the mass effects from the dynamics of relativistic, non-perturbative QCD, we can study systems with one or more heavy quarks (strange, charm, bottom), and compare them with systems made only of light quarks.

A large contribution to baryon and meson masses comes from spin-dependent forces, which are inversely proportional to quark masses. The large mass difference between the $\pi$ (135 MeV, quark spin antiparallel to the spin of the antiquark) and the $\rho$ meson (770 MeV, parallel spins), progressively gets smaller when we replace the $u, d$ quarks with $s, c, b$ quarks.

The mass of ground state hadrons can be described quite well by the following formula:

$$M(q\bar{q}; qqq) = \Sigma_i \, m_i + \Sigma_{i>j} \, \frac{\vec{\sigma_i} \cdot \vec{\sigma_j}}{m_i \, m_j} \, v_{ij}^{hyp} \tag{51}$$

where $m_i$ are the so called constituent quark masses, larger than the bare masses, and $v_{ij}^{hyp}$ is a hyperfine interaction with different strengths, but the same flavour dependence. The success of the constituent quark model is not fully understood by theory [827].

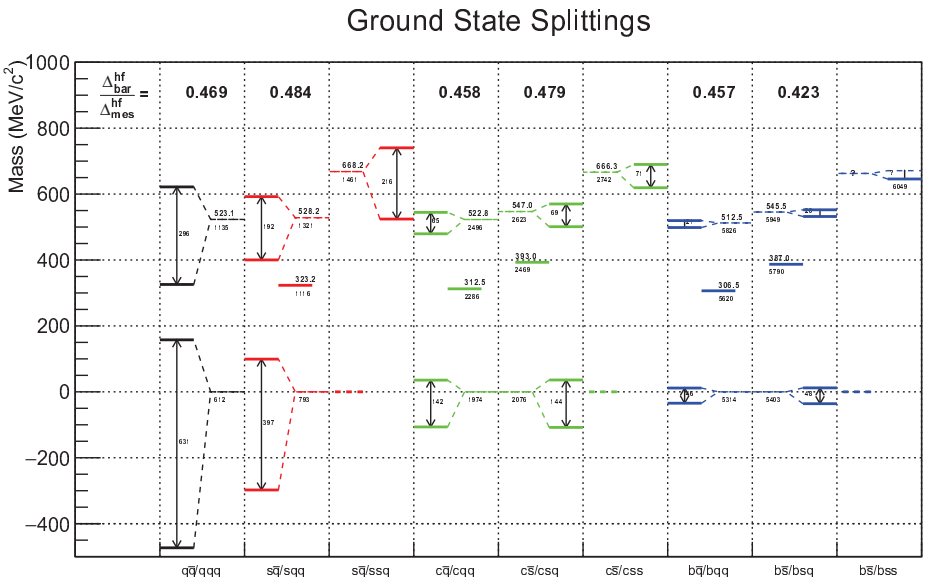


**Fig. 96:** $S$-wave meson and baryon mass splittings

Figure 96 summarises the current understanding of most $S$-wave mesons and baryons. For these hadrons, the measured mass depends only on the mass of the valence quarks and their spin alignment. For baryons, we can sort them assuming that the two lighter quarks are either in a spin singlet state (scalar diquark) or in a spin triplet state (vector diquark). In this second case, the diquark spin can either be antiparallel ($J = 1/2^+$) or parallel ($J = 3/2^+$) to the quark spin. Figure 96 shows baryon-meson mass splittings, calculated relative to the spin-weighted average of the S-wave mesons. A remarkable scale invariance can be observed after averaging out spin effects. HQET predicts that the hyperfine splittings in mesons scale with $1/m_Q$. The same happens with baryons, and the ratio is constant within 10 percent, as we span from strange to bottom [828].

If we average out spin effects, all baryons can be modeled within a few percent as diquark-quark systems. The exchange of a $\bar{u}, \bar{d}$ antiquark with an antisymmetric $ud$ diquark shifts the energy up by about 315 MeV, independent of the heavy quark ($s, c, b$). This shift is about 75 MeV higher if the light

antiquark is replaced by an antisymmetric $sq$ diquark. If the light antiquark is replaced by a vector diquark, the shift is 520 MeV (547 for a vector $qs$ diquark). The scale independence is even more impressive when a $\bar{s}$ is replaced by a $ss$ diquark: the spin averaged splitting is 668 MeV when the third quark is a $u, d$ type, and 666 when it is a charm quark. In the bottom strange system, the $J^P = 3/2^+$ partner of $\Omega_b'$ has not yet been observed, while the $\Xi_b'$ doublet has recently been observed by LHCb [829]. The doubly heavy baryons $ccq$, $bbq$ have not been observed yet. An early claim by experiment SELEX at Fermilab [830, 831] has not been confirmed by the B factories [832, 833] or hadron [834] colliders. But the search is not over, as suggested by the unexpectedly large rate of production of double charmonium at Belle [835] and Babar [836]. In the coming years, LHCb and Belle-II are likely to discover the doubly heavy baryons.

Both for mesons and baryons, the analysis of $P$-wave excitation spectra is made difficult by the large width of many states, both in the light and heavy-light systems. The quantum numbers of spin triplet (singlet) $P$-wave $q\bar{q}$ states are $0, 1, 2^{++}(1^{+-})$. The identification of the multiplet of scalar mesons that can be formed by $u, d, s$ quarks has been a problem for theory since a long time: a recent paper [837] confirms the resonant nature of the broad $\sigma$ and $\kappa$ states, that can form a nonet with inverted mass hierarchy, with the $a_0(980)$ and $f_0(980)$ states, as suggested in reference [821], using the tetraquark model.

$P$-wave $D$ mesons can be modelled by grouping the four state in two doublets, the lightest (heaviest) with the $u, d$ type quark with total angular momentum $j_q = s + l_q = 1/2\ (3/2)$. We expect then two broad states with quantum numbers $J^P = 0^+, 1^+$, and two narrow states with quantum numbers $J^P = 1^+, 2^+$, whose single pion decay to $D^*$ is suppressed by the angular momentum barrier, as the pion is emitted in d-wave. This pattern is observed in the $D$ mesons, but is not observed in the $D_s$ mesons, as the $0^+$ and $1^+$ members, discovered by Babar [838] and CLEO [839], are below the $DK$ and $DK^*$ thresholds, and their hadronic decay is therefore forbidden. We have then a set of four narrow states. A similar pattern should be observed with $B_s$ mesons.

### *7.4.2 Heavy Quarkonium: Charmonium, Bottomonium and $B_c$*

In the literature, heavy quarkonia are described as mesons with a $c\bar{c}$, a $b\bar{c}$, or a $b\bar{b}$ pair . While charmonium was discovered in 1974 (the November revolution), and bottomonium in 1977, the discovery of the ground state $B_c$ is quite recent [840], and the study of the spectroscopy of its excited states has just started. Among all mesons, charmonium and bottomonium have the richest spectrum of states.

The known spectrum of charmonium and bottomonium is shown in Fig. 97, in comparison with the $D_s$ and $B_s$ meson spectra. While all $S$ and $P$-wave states below the open charm threshold have been discovered, the $D$-wave states are now a very active field of research. The most recent progress in the spectrum of narrow charmonia is the discovery of the long sought $\psi(1^3D_2)$, the $J = 2$ partner of the $\psi(3770)$ in the $D$-wave triplet, which decays into $\gamma\,\chi_c$, observed by Belle in $B$ decays [841]. This state is very narrow even if it is above the $D\bar{D}$ threshold, as its quantum numbers $(2^{--})$ forbid its decay to $D\bar{D}$.

The two $D$-wave states with quantum numbers $2^{-+}$ and $3^{--}$ are the last missing pieces of the $c\bar{c}$ spectrum below the open charm threshold.

Besides many states with total widths below 1 MeV, it is quite noticeable to observe that the broadest charmonium state below threshold is actually the $\eta_c$(1S), i.e. the ground state of the whole system, which has a total width of $(32.2 \pm 0.9)$ MeV [81].

The bottomonium spectrum is shown in Fig. 97: we expect to have 3 $S$-wave and 3 $P$-wave multiplets below the open flavour threshold. A major breakthrough in our understanding of bottomonium spectrum occurred in the last decade: all spin singlet states were discovered after 2007, starting from the $\eta_b(1S)$, found by BaBar [842, 843]. In 2010, the simultaneous observation by Belle of $\eta_b(1, 2S)$ [844] and $h_b(1, 2P)$ [845] was made possible only by the experimental observation of a new pathway from

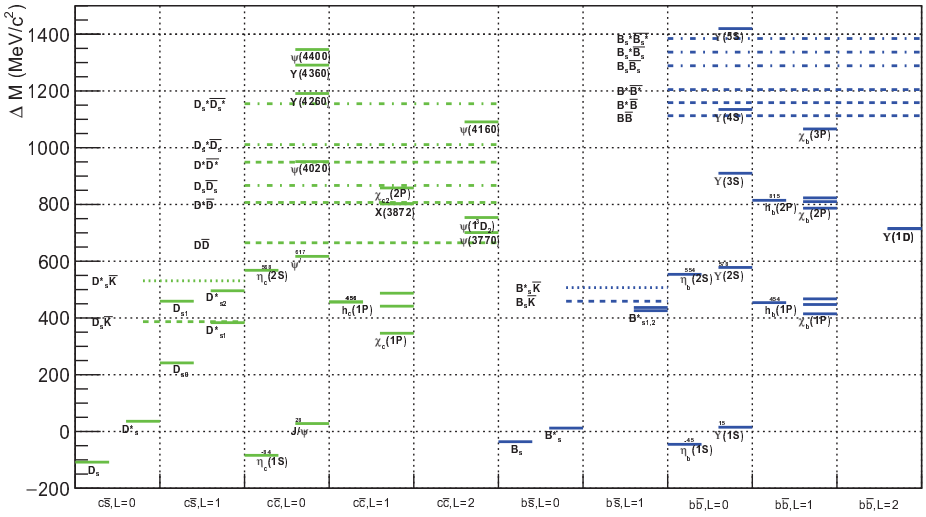


**Fig. 97:** Spectra of charmonium and bottomonium ($S$, $P$, $D$-wave), compared with $D_s$ and $B_s$ mesons ($S$, $P$-wave)

the $\Upsilon(5S)$ state, via two charged bottomonia, which will be described in the next subsection. More recently, Belle discovered that the largest transition from the $\Upsilon(4S)$ to narrow bottomonia is actually an $\eta$ transition to $h_b(1P)$: this is the first ever observed $S$-wave $\eta$ transition, and is by far much stronger than the $\eta\Upsilon(1S)$ and the $\pi\pi\Upsilon(1S)$ transitions. The quantitative understanding of the strength of these transitions remains a challenge for theorists.

After this series of discoveries, we can calculate the hyperfine splittings in bottomonium for $1S, 2S$ and $1P, 2P$ states: the results are summarised in Table 28.

| $\Delta M_{hf}$ | n=1 | n=2 |
|---|---|---|
| S-wave: $M(\Upsilon) - M(\eta_b)$ | $62.3 \pm 3.2$ | $24 \pm 4$ |
| P-wave: $M(\chi_{cog}) - M(h_b)$ | $0.7 \pm 1.1$ | $0.2 \pm 1.3$ |

**Table 28:** Hyperfine splittings in bottomonium (MeV).

The $P$-wave splittings are calculated using $M(\chi_{cog})$, the spin weighted average of the $\chi_b$ states, and are consistent with zero, as we expect from the one gluon exchange potential. The $S$-wave splitting is quite a challenge for theorists. For the ground state, the experimental result is consistent with lattice predictions [846], and in slight tension with the pNRQCD prediction [847].

The hyperfine splitting ratio $r_{hf} = \Delta M_{hf}(2S)/\Delta M_{hf}(1S)$ is $0.412 \pm 0.012$ in charmonium and $0.38 \pm 0.07$ in bottomonium. A lattice prediction of $r_{hf}(b\bar{b})$ is consistent with the existing result. We can then compare the spin averaged $1P - 1S$ splitting for $c\bar{c}$ and $b\bar{b}$ and we obtain $457.5 \pm 0.3$ for charmonium and $453.3 \pm 1.3$ for bottomonium. Remarkably, also these splittings are independent of the hard scale.

Also in bottomonium the $D$-wave multiplet is still unresolved, and the spin singlet state $\eta_{b2}(1D)$ has not yet been found. CLEO discovered a mixture of spin triplet $\Upsilon(1D)$ states in 2003 [848], and further confirmations came from Babar and Belle. $\Upsilon(1D)$ can be reached from both $3S$ and $4, 5S$ states. The $\chi_b(3P)$ multiplet was discovered recently by ATLAS [849] and is also being studied by its LHC competitors, CMS and LHCb [850]; the production of $\chi_b(3P)$ in radiative or hadronic transitions from the $\Upsilon(4, 5S)$ is currently being studied by Belle at KEKB.

Many missing states are close to the open bottom thresholds: $\eta_b(3S)$, $h_b(3P)$, all $\Upsilon(2D)$ states, and even the $\Upsilon(1F)$ multiplet, expected around 10350 MeV/c$^2$.

The last frontier of heavy quarkonium studies is the spectrum of $B_c$ mesons, discovered in 1998 by CDF [840]. More recently, thorough studies on these states are being performed by LHC experiments:

- ATLAS observed a combination of the two S wave radial excitations. In the meantime, the vector $B_c^*$ state, which is dominantly expected to decay to $B_c$ and one $M1$ photon, is still unobserved.
- LHCb has performed state-of-the-art measurements of the mass of the ground state, using a variety of new channels.

The spectrum of excitations of the $B_c$ meson is completely unexplored and it will be a challenging task for the collider experiments at LHC.

### *7.4.3 Multiquark systems*

The discovery of X(3872) in B decays at Belle [851] came quite unexpectedly, and its confirmation by CDF in prompt production at the Tevatron attracted a large amount of theoretical interest on this state. Some authors believe that strong interaction analogs of Van der Waals forces could generate potentials binding hadron molecules. However, several issues about their production mechanism at hadron colliders have been studied [852,853]. After more than a decade from this discovery, we know that the X(3872) has quantum numbers $J^{PC} = 1^{++}$, and its width is narrower than 1.2 MeV, but its nature is still uncertain. It could either be a mixture of a charmonium state (the $\chi_{c1}(2P)$ ) and a $D\bar{D}^*$ molecule, or a tetraquark.

One year after, Babar observed another exotic state [854] with vector quantum numbers, the $Y(4260)$, decaying to $J/\psi\pi\pi$ in exact correspondence with a steep drop of the $c\bar{c}$ cross section. Soon after, Belle discovered two more vectors at $E_{cm} = 4.36$ and 4.66 GeV, decaying to $\psi'\pi\pi$. Recently, BES-III has reported the observation of radiative transitions between the $Y(4260)$ and the $X(3872)$, a discovery that may hint at a common nature of these two states.

After the discovery of the $Y(4260)$, Belle started a massive campaign of studies to search for the bottomonium counterpart of this state, triggered by the observation of very large yields of dipion transitions to $\Upsilon(1,2,3S)$ from the proximity of the peak of the $\Upsilon(5S)$ resonance. This study yielded the discovery of the two spin singlet P wave states, $h_b(1,2P)$ described in the previous chapter, but, most important, it also represented the first observation of two charged bottomonium states, dubbed $Z_b(10610)$ and $Z_b(10650)$, in close proximity to the $B\bar{B}^*$ and $B^*\bar{B}^*$ thresholds. Charged states were explicitly predicted by compact tetraquark models [855] and have a clear role in the picture proposed in [822]. The discovery of heavy charged multiquark systems has further ignited a renewed theoretical interest in the field of hadron spectroscopy [856, 857].

Soon after, Belle and BES-III discovered the charged charmonium states $Z_c(3900)$ and $Z_c(4020)$, in the proximity of the $D\bar{D}^*$ and $D^*\bar{D}^*$ thresholds. As in the case of the $Z_b$ states, which are reachable via single pion transitions from the $\Upsilon(5S)$, the $Z_c$ states can be reached via single pion transitions from the $Y(4260)$ and the $Y(4360)$. A difference between $Z_c$'s and $Z_b$'s can be found in the decay patterns: While both $Z_b$'s decay with comparable $BR$'s to all $1^{--}$ and $1^{+-}$ narrow bottomonia, the $Z_c(3900)$ decays preferentially to $\pi J/\psi$ and the $Z_c(4020)$ prefers $h_c\pi$.

A thorough program of studies is underway at BES-III to investigate the nature of the charged charmonia, and the exotic charmonium-like states. Future prospects of studies at Belle-II will include the search for the doubly charmed meson $T_{cc}$, with quark content $cc\bar{u}\bar{d}$.

### *7.4.4 Hybrids*

Hybrids, i.e states containing both quark and gluon excitations, have been studied in various models [858–863], but recent lattice simulations [864–869] have generated greater expectations [869]. More-

over, on the experimental side, in recent years (see the previous subsection) several new states, in particular in the charmonium spectrum, have been discovered. These probably include a hybrid resonance, the $Y(4260)$, discovered by Babar [854].

Conventional heavy quarkonia are well described by non-relativistic QCD, so that one can expect that hybrids containing heavy quarks could be treated in a similar way, i.e. by considering gluon excitations in the presence of slow quarks. Moreover, in the physical gauge, the dynamical gluons can be separated from the instantaneous Coulomb-type forces that act between color charges; thus, while the non-abelian Coulomb potential is expected to be responsible for binding and confinement, the remaining, transverse gluon excitations could contribute to the spectrum. In non-relativistic, physical gauge QCD, the lowest mass charmonium hybrid multiplet has been predicted to be composed by the states with quantum numbers $J^{PC} = 1^{--}$; $(0;\ 1;\ 2)^{-+}$ [870]. This four-state hybrid multiplet identified in physical gauge calculations, has been recently identified also in lattice simulations [867–869], both in the heavy [867, 868] and light quark sectors [869]; moreover, it includes an exotic state (a state with exotic quantum numbers) with $J^{PC} = 1^{-+}$.

In the non-relativistic, physical gauge QCD the lowest mass charmonium hybrid multiplet can be explained as due to a color-octet $c\bar{c}$ pair with ${J_q}^{P_q C_q} = 0^{-+}$ or $1^{--}$ corresponding to the total quark-antiquark spin with $S_q = 0$ and $S_q = 1$, respectively, coupled to a single physical, transverse gluon with predicted quantum numbers $J_g^{P_g C_g} = 1^{+-}$ [870, 871]; the unusual positive parity of the physical gluon originates from the non-abelian nature of the Coulomb interactions as explained in Refs. [870, 871]. It will be important to study both experimentally and theoretically all their possible decays that distinguish them from ordinary quark antiquark states [872].

Meson Spectroscopy is a powerful tool to answer fundamental questions in QCD, like the origin of color confinement and the role of gluons inside hadrons. Mesons are the simplest quark bound system and, therefore, the ideal laboratory to study the strong force at the non-perturbative energy scale of a few GeV. In particular, unconventional mesons would be the best experimental evidence of the active role of gluons in hadron dynamics. In this respect, from an experimental side there will be dedicated experiments at CERN, as well as at Jlab, FAIR, BES and Belle. New high-statistics and precise data need an adequate analysis [872, 873]. Beyond providing a deeper understanding of the inner workings of non-perturbative QCD, theoretical control over hadronic final-state interactions is also essential for the hunt of physics beyond the Standard Model.

### 7.5 Total, elastic and diffractive cross sections

When two hadrons collide, inelastic processes contribute to around 50% of the cross section. The remaining almost-half of the total cross section is due to elastic (around 25%) and (mainly soft) diffractive processes. The latter ones are characterised by the exchange of a color-singlet object (historically known as Pomeron) resulting in the dissociation of one (single diffraction) or both (double diffraction) of the incoming hadrons, which are scattered at very small angles and carry most of the initial energy. Investigating the region very close to the outgoing beams is therefore mandatory for a measurement of the total cross section and complementary to studying the central region surrounding the collision point.

Because it involves the detection of the elastically or diffractively scattered protons, measurements of the total and of the elastic cross sections, as well as that of diffractive processes, require full rapidity coverage and special engineering solutions to access the primary vacuum of the machine. For the first issue, trackers and calorimeters have to be placed in the "forward" regions surrounding the beam pipe; for the second one, special insertions of the beam pipe (roman pots) are utilised to host detectors to track the scattered protons. At the LHC, only TOTEM and ATLAS-ALFA are at the moment equipped with detectors insertable with roman pots.

In the case of elastic and inelastic interactions, since the cross sections of the involved processes are large, the statistics is usually not a problem. The main uncertainties originate from systematic ef-

fects. For the measurements which require a precise knowledge of the luminosity, the uncertainty on the luminosity itself is the largest error source. It has in fact been proven difficult for the experiments to keep this uncertainty at the level of one percent. Another systematics is related to the incomplete rapidity coverage in the forward region. Usually the experiments are not instrumented at rapidities higher (lower) than about $+5$ $(-5)$, losing the possibility of catching diffractive events at low masses, whose amount has to be extrapolated, introducing therefore a sizeable systematic error. Other systematic effects in the measurement of the elastic and diffractive scattering are related to the machine optics. The kinematics of the scattered protons must in fact be reconstructed from the angle and position of protons which have passed through several machine elements and which are eventually detected in the roman pots, hundreds of meters away from the IP.

### *7.5.1 Total cross section in pp collisions*

The first experimental results on cross sections at hadron colliders date back to the early 1970's with the CERN Intersecting Storage Rings (ISR) which provided $\bar{p}p$ and $pp$ collisions with a center of mass energy of 20 to 50 GeV. During the 1980's and 1990's the experiments at the new accelerators SPS at CERN and Tevatron at Fermilab accumulated data on $\bar{p}p$ scattering at energies from 0.5 to 1.8 TeV. The start of the LHC and its operations at $\sqrt{s} = 7$ and 8 TeV have provided plenty of data which are still being thoroughly analysed. In terms of proton-proton cross sections, the results extend to an unprecedented energy domain. Moreover, the LHC energies begin to overlap with the range of cosmic ray showers, as discussed in Section 7.7.

The measurement of the total cross section can be achieved by measuring the inelastic and elastic rate or, exploiting the optical theorem, the elastic scattering only, provided that the differential distribution is measured at angles small enough (at the LHC it means four-momentum transfer $|t| < 0.5$ GeV$^2$). It has to be noted that the former measurement can be luminosity independent, while for the second one a measurement of the luminosity is mandatory. All the available measurements of the total, elastic and inelastic cross sections are summarised in Fig. 98.

Concerning the total cross section, the rise with the centre of mass energy has been confirmed by the LHC data. This evidence can be interpreted as a proton becoming larger and blacker as the energy increases. Moreover the data, fitted by several authors, favor a $\ln^{\gamma} s$ behavior, with $\gamma$ compatible with 2, which can be seen as a qualitative saturation of the Froissart-Martin bound, since it corresponds to the maximum rate of rise with energy which is allowed by analiticity and unitarity; numerically, the actual data lie well below the bound itself. In particular, the measurements of the total cross section at $\sqrt{s} = 7$ and 8 TeV definitely indicate consistency with a $\ln^2 s$ dependence, as predicted several years ago by the COMPETE Collaboration [874].

Several theoretical models have been developed during the last decades to interpret the experimental results. Unfortunately, the perturbative QCD approach cannot be used in this context since most of the processes contributing to the total cross section are characterised by low momentum transfer. Some of the models are still based on Regge theory, while others prefer using optical or eikonal approaches. Moreover, so-called QCD-inspired models are trying to connect the concepts of Pomeron trajectories and proton opacity to the QCD description of elementary interactions between quarks and gluons. At the moment, no model manages to describe qualitatively and quantitatively the large amount of data available; they all have merits and shortcomings. Typically, they successfully describe the experimental results in a certain kinematic range but completely fail in other ones.

### *7.5.2 Elastic scattering*

The distribution of the four momentum transfer $t$ in elastic scattering (Fig. 99) exhibits a pronounced forward peak which is well described, at first approximation, by an exponential of the form $e^{-B(s)t}$. In general, the overall forward peak ($|t| \lesssim 0.5$ GeV$^2$) does not follow a simple exponential shape,

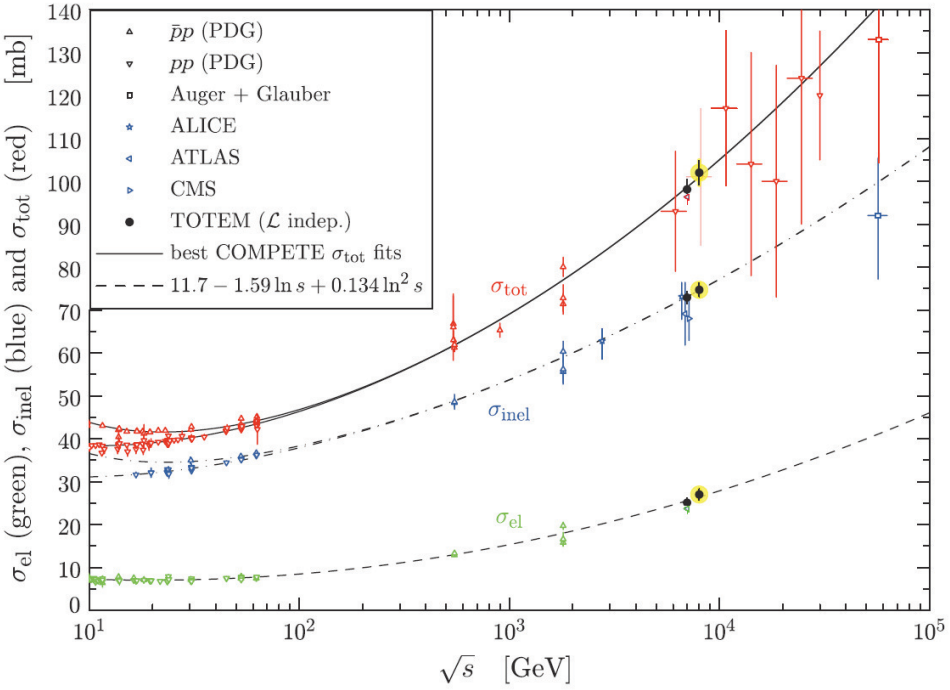


**Fig. 98:** The dependence of total, inelastic and elastic cross sections on the center of mass energy $\sqrt{s}$. The continuous black lines (lower for $pp$, upper for $\bar{p}p$) represent the best fits of the total cross section data by the COMPETE collaboration [874]. The dashed line results from a fit of the elastic scattering data. The dash-dotted curves correspond to the inelastic cross section and have been obtained as the difference between the continuous and dashed fits.

which has important implications in the understanding of the hadronic interactions and of the interference between the hadronic and electromagnetic ones. This aspect is being investigated by TOTEM, whose latest measurements allowed to access the kinematical region where the Coulomb interaction becomes visible.

At larger momentum transfers a diffraction-like structure is observed, followed by a smooth behaviour. The dip appears to recede towards zero with increasing energy at a value of $t$ roughly proportional to $\sigma_{tot}^{-1}$, as suggested by the geometrical picture. Data from $pp$ and $\bar{p}p$ scattering differ considerably in the region where the diffractive structure appears: the former shows a pronounced dip, while the latter actually shows more of a shoulder than a dip.

### *7.5.3 Diffraction*

In diffractive processes in proton-proton collisions, the final state contains one ($pp \to pX$) or both ($pp \to pXp$) of the incoming proton(s) and a hadronic system $X$. Because no quantum numbers are exchanged between $X$ and $p$, one (two) region(s) in rapidity devoid of particles (large rapidity gap, LRG) is (are) the signature of such processes in addition to the scattered proton(s). Diffraction is also observed in the interaction of point-like probes with hadrons, and it has been extensively studied in Deep-Inelastic $ep$ Scattering (DIS) at the HERA collider [875], where, by changing the virtuality of the photon, the size of the probe can be varied at will, spanning the transition from the soft regime, typical of diffractive reactions in hadron physics, to the hard regime, where pQCD becomes applicable. This is the reason why the understanding of diffraction in QCD has received a great boost from the HERA results.

In the pre-LHC era, at HERA, Tevatron (and also at RHIC), tagging the LRG or the outgoing proton(s) provided complementary results (high statistics with the LRG technique, conversely well un-

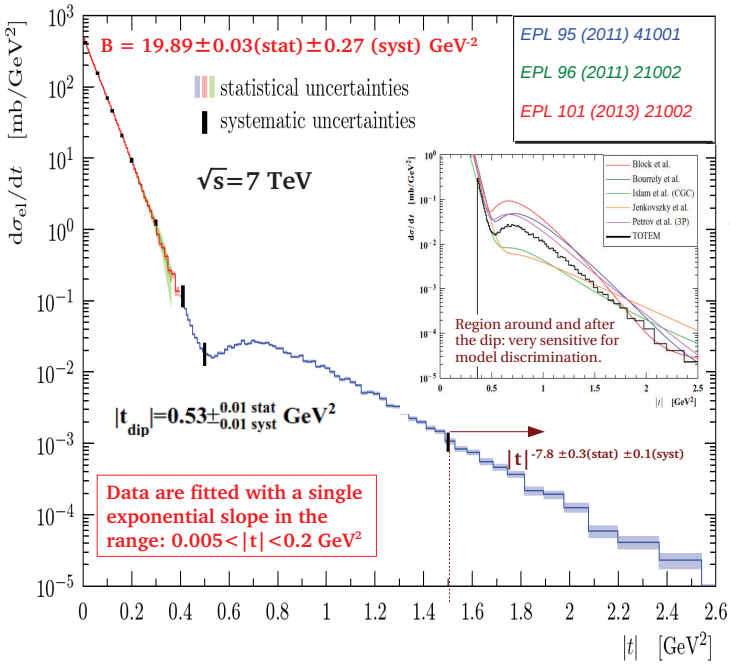


**Fig. 99:** A summary of the TOTEM results for the single differential elastic cross section, $d\sigma_{el}/dt$, at $\sqrt{s} = 7$ TeV.

derstood systematics with the proton taggers). At the LHC, and notably in the case of ATLAS and CMS, the presence of pileup spoils the rapidity gap signature. This made the LRG technique already a challenge with the Run I data (see e.g. [876–878]). LRG measurements will be possible with the forthcoming Run II data in special running conditions [879] or with the LHCb detector, which operates in low-pileup scenario due to special settings and offset leveling techniques. Conversely, measuring diffractive interactions at high luminosity with ATLAS and CMS will be possible only with proton taggers. Both experiments have a program for instrumenting the forward region. In the CMS case, the TOTEM detector, conceptually designed for forward physics as illustrated above, shares the same interaction point. Exploiting the synergy between the two experiments, which started already in 2012 when CMS and TOTEM successfully took common data (the runs were synchronised and the data merged offline), is the heart of the CMS-TOTEM Precision Proton Spectrometer (CT-PPS) project [880], recently approved by the LHCC. It consists of a pixel silicon tracking system to measure the position and direction of the protons, and a set of timing Cherenkov quartz counters to measure their arrival time. The ATLAS Forward Proton (AFP) detector [881] consists of similar devices. They will allow the reconstruction of the mass and momentum of the system $X$ resulting in central exclusive production (CEP) processes, $pp \to pXp$. The mass of the system $X$ depends on the longitudinal momentum losses, $\xi$, of the scattered protons; the acceptance in $\xi$ of the proton taggers in turn depends on the machine optics: protons with any $\xi$ can be detected in TOTEM and ATLAS-ALFA roman pots in special low-luminosity runs (betatron function at the interaction point $\beta^*$=90 m)[22] in which the mass coverage in CEP reactions extends to any $M_X$ as long as $|t|$ of both scattered protons is larger than 0.04 GeV$^2$. This is complementary to the range $M_X \geq 300$ GeV in normal high-luminosity runs. Furthermore, the CEP via a double diffractive channel, with constrained kinematics, provides a unique method to access a variety of physics topics at the LHC, such as new physics via anomalous production of $W$ and $Z$ boson pairs, high$-p_T$ jet production, and possibly the production of new resonances, including a thorough spin analysis and a study of the decay

[22] In terms of the accelerator optics, the value of the betatron function $\beta$ at a point is the distance from this point to the one at which the beam is twice as wide. The lower is the value of $\beta^*$, the smaller is the beam size and thus the larger is the luminosity. In standard LHC runs $\beta^*$ = 0.5 m

modes of glueball candidates, like the $f_0(1710)$, in high-$\beta^*$ runs [879].

A key physics issue in diffractive processes is whether the Diffractive Parton Distributions Functions (DPDFs), introduced as a class of parton distribution functions or fracture functions [882–884]—describing the usual proton PDFs conditional to having a diffractive scattering—are or are not universal, i.e. whether collinear factorisation [885] holds. DPDFs were extracted from high-precision HERA data by performing perturbative QCD fits at next-to-leading order accuracy and including full experimental and theoretical error estimations [875, 886–888]. Support of factorisation was provided by analyses of diffractive di-jet cross sections in DIS which, despite large theoretical errors, are well described by next-to-leading order predictions based on DPDFs extracted from the inclusive diffractive DIS data [889]. However, hard scattering factorisation was proven to fail in $p\bar{p}$ collisions at the Tevatron [890, 891], where single diffractive production cross sections of di-jet and electro-weak bosons are overestimated by an order of magnitude by predictions based on HERA DPDFs.

The factorisation theorem is at the heart of modern QCD phenomenology at hadron colliders. It provides crucial predictivity to the theory and, so far, has been tested and verified by all phenomenological analyses. Understanding the mechanism, still unknown, responsible for the striking breaking of factorisation in hard diffraction would unveil the non-perturbative phenomena behind it. There are other processes at the LHC which may substantially improve our knowledge, namely the single diffractive Drell-Yan process. A measurement of the dependence of the cross section on the invariant mass of the di-lepton pair would be very informative. This analysis would reveal if the factorisation breaking mechanism depends on $Q^2$, and appropriate ratios to the inclusive Drell-Yan cross sections could spot this eventual dependence in a model independent way. In the simplest scenario in which the single diffractive cross section is scaled by a common factor, independent of $Q^2$, it would be extremely interesting to estimate to what extent the partonic structure of the diffractive exchange (encoded in the DPDFs) is altered in hadronic collisions with respect to diffractive DIS. For this purpose, it will be mandatory to select kinematic ranges of the proton energy loss $\xi$ and of the lepton-pair rapidity (and therefore of the DPDFs fractional momentum $\beta$) corresponding to regions in which the DPDFs have been determined in diffractive DIS with sufficient precision. Since the Drell-Yan process is essentially a quark-dominated process, this measurement should be complemented by the study of other processes sensitive to the (dominant) gluon DPDF, such as single diffractive prompt photon and di-jet production.

High transverse momentum production of jets and/or photons in photon-Pomeron interactions can be measured if the full kinematics of final state protons can be reconstructed, since photon and Pomeron emissions from protons are expected to populate different regions of the $t$ spectrum. If this measurement turns out to be feasible, the LHC machine could possibly offer the answer to the unsolved question raised in diffractive di-jet photo-production at HERA. To conclude, the hard diffraction program at LHC can address fundamental issues in our understanding of non-perturbative phenomena in high energy hadron interactions and investigate in detail the only case in which factorisation, at the heart of QCD phenomenology, is strikingly broken.

### 7.6 Multi-parton interactions

In collisions with large momentum transfer exchange, the interaction between hadronic constituents is localised in regions in transverse space much smaller than the hadronic dimension. On the other hand, at high energies and relatively low $p_t$, hard collisions contribute to a finite fraction of the total inelastic cross section. In such a regime, the hard component of the interaction may be disconnected in transverse space. The process is thus given by the incoherent sum of weakly correlated hard and semi-hard subprocesses and is called Multiple Parton Interaction (MPI).

When the hard component of the interaction is disconnected, the hard process is initiated by several pairs of partons. The cross section is hence characterised by a much stronger dependence on the incoming parton flux, as compared with the familiar case of hard processes originated by just a single pair of partons. MPI become therefore more and more important when increasing the centre of mass energy of

the colliding hadrons, where partons with smaller and smaller fractional momenta play an active role. Another general feature is that MPI are characterised by at least one non-perturbative scale, related to the typical transverse distance between the hard interaction regions. A direct consequence is that MPI cross sections decrease much faster, as a function of transverse energy, as compared with usual large $p_t$ single scattering parton interactions. MPI are further characterized by peculiar correlations. Final state partons generated by a connected hard interaction are in fact highly correlated in transverse momenta and rapidities. Disconnected hard interactions produce various groups of highly correlated partons in the final state, while correlations between partons belonging to different groups are weak.

All state-of-the-art Monte Carlo event generators need in fact to include MPI in order to be able to reproduce the global features of inelastic events (final state multiplicities, energy densities, etc.). In almost all cases MPI are implemented by assuming a Poissonian distribution of elementary partonic interactions, with average number depending on the impact parameter of the hadronic collision [892]. Specific conjectures, concerning in particular the actual distribution of initial state partons in transverse space, the regularisation of the elementary partonic interaction at low transverse momenta and hadronisation, depend on the specific assumptions in the different Monte Carlo codes. The non-perturbative component of MPI combined with the contribution to the final state due to soft radiation and to the fragmentation of initial state remnants, cannot be completely separated from each other, in such a way that the resulting quantitative information on MPI is unavoidably rather uncertain even if several decompositions have been attempted based on topological constraints and specific selections of final states [893–895].

In this respect, a cleaner understanding of the different dynamical mechanisms, taking place in the relatively low $p_t$ region, can be obtained by direct observation of MPI processes. In the simplest case, Double Parton Interaction (DPI), the general features characterising MPI are summarized in the 'pocket formula' of the corresponding inclusive cross section [896]:

$$\sigma_{double}^{(A,B)} = \frac{m}{2}\frac{\sigma_A \sigma_B}{\sigma_{eff}}\,, \tag{52}$$

where $A$ and $B$ label the two elementary partonic processes, localised in two different disconnected regions, $m$ is a symmetry factor ($m = 1$ if $A$ and $B$ are identical processes and $m = 2$ if $A$ and $B$ are different), $\sigma_A$ and $\sigma_B$ are the two cross sections to observe inclusively either the process $A$ or the process $B$ in the same hadronic collision. All unknowns in the process converge into the value of a single quantity with the dimensions of a cross section, $\sigma_{eff}$. Actually, when hard interactions are rare, the probability to have the process $B$ in an inelastic interaction is given by the ratio $\sigma_B/\sigma_{inel}$. Once the process $A$ takes place, the probability to have the process $B$ in the same inelastic interaction is different. It can anyway be always written as $\sigma_B/\sigma_{eff}$, where $\sigma_{eff}$ plays *effectively* the role, which was of the inelastic cross section in the unbiased case.

Double-PDFs encode information on the correlations between two partons inside a target and represent the non-perturbative contribution to the hadron structure, not accessible in a single-scattering large-$p_t$ interaction [897]. One may thus expect $\sigma_{eff}$ to depend on all the different observables characterising the process. Conversely, it is remarkable that, although more precise measurements are expected to reveal some dependence of $\sigma_{eff}$ on the reaction channel and on the kinematical regime, Eq.(52) has shown to be able to describe the experimental results of the direct search for DPI in rather different kinematical regimes [898–902] with a value of $\sigma_{eff}$ compatible with a universal constant (see Fig. 52). Even though the value of $\sigma_{eff}$ is still rather uncertain, the actual experimental evidence is that its value is much smaller than $\sigma_{inel}$ (roughly by a factor 4), which represents a rather clear indication of the presence of important correlations in the hadronic structure. On the other hand, the experimental study of DPI in $pp$ collisions can only provide limited information. In particular it cannot provide a suitable understanding of the small observed value of $\sigma_{eff}$.

A handle to obtain additional information is provided by DPI in $pA$ collisions [903]. The dynamics of DPI is in fact different in $pp$ and in $pA$ collisions. In addition to the process where DPIs take place between the projectile proton and a given target nucleon, in $pA$ DPIs can in fact also occur between the

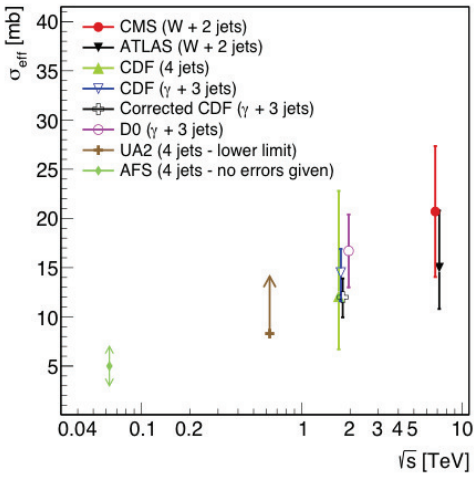


**Fig. 100:** Different experimental results on the value of $\sigma_{eff}$

projectile and two different target nucleons. While the first contribution to the cross section is proportional to $A$ and is very similar to DPI in a $pp$ collision, the second contribution is proportional to $1/R^2$, where $R$ is the nuclear radius, and grows with $A$ as $A^{4/3}$. The second contribution therefore introduces a rather strong anti-shadowing correction to the first one, which may be of the order of 200-300% in the case of $p-Pb$ collisions. Moreover, while the first contribution, linear with $A$, is proportional to $1/\sigma_{eff}$ and it is therefore related to the typical transverse region, where the two elementary hard interactions take place, the second contribution, being proportional to the inverse nuclear radius squared, is practically independent, in the case of heavy nuclei, of the distance between partons in transverse space. Its contribution to the cross section is therefore directly proportional to the multiplicity of pairs of partons in the projectile, which can thus be estimated by measuring the amount of anti-shadowing in DPI in $pA$ collisions. DPI in $pA$ collisions can therefore provide valuable indications on the multiplicities of parton pairs in the hadron at different fractional momenta. By comparing with the measured value of $\sigma_{eff}$ in $pp$ collisions one therefore obtains indications on the corresponding typical transverse distances between the interacting parton pairs. One should also emphasise that, in this way, one has access to unprecedented information on the three dimensional partonic structure of the hadron.

Reducing substantially the experimental errors in the measurement of $\sigma_{eff}$ is required as well as measuring the dependence of $\sigma_{eff}$ on $Q^2$ and on fractional momenta in different reaction channels and different kinematics, while quantifying the amount of anti-shadowing in DPI in $pA$ collisions in the same reaction channels and regimes. Both high luminosities, in order to significantly increase statistics, and high centre of mass collisions energies, to increase the parton flux and thus the relative rate of MPI, are key issues. From the theory side further efforts are needed to unravel features of DPI, which are still a matter of debate (the relevance of the contribution of the interplay region between connected and disconnected hard interactions [904], the role of spin and color [905]).

A clear indication on the dependence of $\sigma_{eff}$ on transverse momenta will provide valuable indications on the deviations from the Poissonian distribution of elementary partonic interactions to be included in the Monte Carlo event generators, improving in this way the physics content and reducing the space to phenomenological assumptions, affecting in particular the relative importance of radiation with respect to MPI in the description of the inelastic event.

A relevant point is finally that an accurate determination of the value of $\sigma_{eff}$, for different processes and kinematics, will allow accurate estimates of the backgrounds due to DPI in various processes of interest in the search for new physics. The contribution of MPI is in fact expected to become signifi-

cant, when looking at various processes that are absent, at leading order, in the Standard Model [906].

## 7.7 Cosmic rays and the impact of collider experiments

A precise modeling of the properties of hadronic interactions is mandatory to understand and interpret correctly the showers generated by cosmic rays in the Earth's atmosphere and in other astrophysical environments related to dark matter searches or neutrino physics. Uncertainties on cross sections and on the properties of particle production in hadronic collisions are indeed in several cases the main source of systematic error in measurements of great interest. An appropriate program of measurements with accelerators beams could provide the information to reduce the systematic errors to a level that would significantly enhance the scientific value of existing and future observation programs.

### *7.7.1 High Energy Cosmic Rays*

The energy spectrum of cosmic rays (CR) covers a very broad energy range, at least up to $E \simeq 10^{20}$ eV, with an intensity that decreases rapidly with energy, approximately as a power law ($\phi(E) \propto E^{-\alpha}$) with an exponent $\alpha$ between 2.7 and 3.3. CR direct observations with detectors placed above the Earth's atmosphere on balloons or satellites are only possible in the low energy region, where sufficient statistics can be collected. Above an energy of order $E \simeq 10^{14}$–$10^{15}$ eV, the CR spectrum and mass composition can only be estimated by indirect methods, from the observation of the extensive air showers generated in the atmosphere by the primary particles (most of the high energy particles are protons of fully ionised nuclei).

The reconstruction of the energy and identity (mass number) of the primary particle from the shower observables requires a sufficiently precise description of the relevant properties of hadronic interactions, and uncertainties in their modeling are the main source of systematic error. An example is given in Fig. 101, where data obtained by the Auger detector [907] on $X_{\max}$ (the column density of air where the longitudinal development of a shower has its maximum) are shown. The different lines in the figure illustrate, as a function of energy, the theoretical predictions on $\langle X_{\max}(E)\rangle_{p,\mathrm{Fe}}$ for proton and iron showers, obtained with different Monte Carlo models. The spread among the lines gives a rough indication of the present uncertainties on the modeling of the shower development, and of their impact in the interpretation of the data. The reduction of such theoretical systematics would allow a better determination of the CR average mass (as a function of energy), with important consequences on the understanding of their origin and propagation. Similar considerations apply also to the low energy range ($E \simeq 10^{15}$–$10^{18}$ eV), where the energy spectrum shows features (the most prominent being the so called "knee") that should be better described and understood.

The laboratory-frame energy range $10^{15}$–$10^{20}$ eV corresponds, for a proton primary particle, to nucleon–nucleon interactions with centre-of-mass energy in the interval $\sqrt{s} = 1.4$–430 TeV, that extends far beyond the maximum energy available at LHC. The study of the highest energy CR requires therefore an extrapolation of the results obtained in accelerator experiments. Detailed studies performed at the highest energy available at LHC play a crucial role in reducing the uncertainties associated with this extrapolation.

CR showers develop in air, where the target is formed by nuclei (Nitrogen, Oxygen and Argon) with mass numbers $A = 14$–18, while the primary cosmic rays consist of protons and fully ionized nuclei, with a mass number distribution that extends up to elements in the iron group ($A \lesssim 56$). The shower modeling therefore requires a good understanding of hadron-nucleus and nucleus-nucleus collisions with the mass number of the target and projectile nucleus in the quoted intervals.

One infers from the discussion above that measuring hadronic interaction properties in $pp$ and $\bar{p}p$ collisions is fundamental. The recent results on the total and elastic cross sections by TOTEM, ALICE, ATLAS and CMS at $\sqrt{s} = 7$ and 8 TeV, discussed in Section 7.5, are very informative as they cover an unprecedented energy range, and even more so will be the future Run II measurements. With the caveat

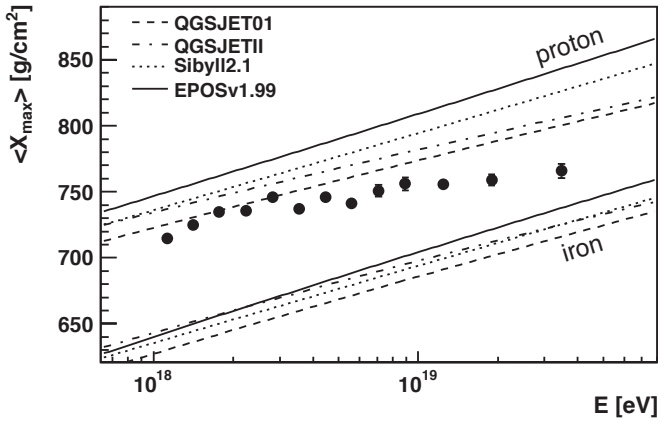


**Fig. 101:** Average $X_{\max}$ measured by the Auger experiment [907] compared with air shower simulations using different hadronic interaction models.

that to use such results for the modeling of CR showers one needs to apply corrections based on a good understanding of nuclear effects. Obtaining measurements for $p$-nucleus and nucleus-nucleus scattering would be highly desirable. The properties of meson-nucleus collisions are also important because high energy $\pi^{\pm}$ and kaons produced in the cascades have a small decay probability, and interact.

The development of CR air showers is driven by the interaction lengths of the particles and by average properties of particle production, such as inclusive energy spectra and multiplicity distributions. Therefore, in most CR studies the rare, hard processes that are the main interest and motivation in accelerator experiments are of little importance. The secondary particles generated in the collisions that are most important for the shower development are those carrying large energy in the laboratory frame and control the energy flow. These particles correspond to the projectile fragmentation region ($x_F \gtrsim 0.1$), and are unfortunately very difficult to measure in collider experiments because they emerge at very small angle with respect to the beam direction. At LHC the beam fragmentation regions, i.e. those at large pseudorapidity $|\eta|$, are studied by detectors such as TOTEM, CASTOR and LHCf. The LHCf experiment has a short-medium term plan which foresees to repeat at 13 TeV the Run I measurements on neutral-particle (neutral pions, gammas and nucleons) production cross sections in the very forward region of proton-proton and nucleus-nucleus interactions. A plan has been presented to perform similar studies at RHIC with 500 GeV $pp$ collisions [908] and with proton-nucleus collisions [909].

The study of collisions using the extracted LHC beam on a fixed target could also be very valuable. A possible scheme for beam extraction is the technique of crystal channeling [910], proposed in the CRYSBEAM project (ERC CoG, funded), where the strategy is to direct the LHC beam on an instrumented absorber made of light materials (carbon, nitrogen, oxygen,..) emulating the Earth atmosphere composition. Also studies at lower energy (for example with a beam extracted from the SPS accelerator) would allow measurements useful for a reduction of the systematic uncertainties on shower development. In this context it seems very interesting to have an experimental program associated to an extraction of the LHC proton beam [911] (using perhaps techniques such as those discussed in [912]).

### *7.7.2 Galactic cosmic rays and cosmic antimatter*

As discussed in the previous subsection the galactic cosmic rays observed with direct measurements span an energy range from about tens of MeV up to hundreds of TeV, and include protons, iron and nickel nuclei, antiprotons, leptons and $\gamma$-rays. The interpretation of galactic cosmic ray data requires, as well as the correct modeling of their sources and of the turbulence spectrum of the galactic magnetic

field, also the knowledge of the cross sections that regulate the production and destruction of cosmic rays interacting with the interstellar medium. For many production and inelastic cross sections, data are scarce or completely missing.

In particular, the *antiprotons* in the Galaxy are of secondary origin and are produced by the scattering of cosmic protons and helium nuclei off the hydrogen and helium in the interstellar medium. The only measured production cross section is the proton-proton one, while all the reactions involving helium have no laboratory data in the useful antiproton energy range ($\sim$ 0.1-100 GeV) [913, 914]. The empirical modeling of those cross sections induces an uncertainty in the antiproton flux of about 30-40%. This should be compared with the $\sim 10\%$ accuracy expected for the forthcoming AMS-02 data on the antiproton flux. The interpretation of the data collected in space will be likely limited by the lack of laboratory measurements!

Accurate knowledge of the cosmic antiproton flux is not only useful to the understanding of the origin and propagation of galactic cosmic rays, but also to the indirect dark matter searches, as will be discussed in the next subsection. The secondary antiproton flux acts as a background when looking for a dark matter signal in the observed antiproton flux.

We emphasise here the need for a dedicated experiment aimed at measuring the exclusive cross section $p + \mathrm{He}$, with particular interest for the channel $p + \mathrm{He} \rightarrow \bar{p} + X$. This measure would also reduce the uncertainties in the predictions of cosmic *antideuterons*. Having the higher signal-to-background ratio, antideuterons are considered at present the most favoured indirect dark matter channel.

As for the scattering $p + \mathrm{He}$, we stress the importance of the measurement of the exclusive cross section. We notice that the knowledge of the cross section for $\gamma - rays$ from the neutral pions produced in $p + \mathrm{He}$ scattering is of relevance for the modeling of the galactic emission [915] and therefore the interpretation of the plethora of data taken by the Large Area Telescope (LAT) on the Fermi Gamma-ray Space Telescope (Fermi). A better modeling of the $\gamma$-rays from hadronic reactions, and in particular the ones involving scattering on helium, would improve the power of the indirect dark matter searches through $\gamma$-rays and the study of the origin of cosmic rays.

A dedicated experiment with a beam of protons accelerated at CERN to energies of a few GeVs and scattering off a helium target would therefore be of the utmost importance in the effort to understand the mystery of dark matter in the Universe and the origin and propagation of cosmic rays in the Milky Way. More generally, an extensive laboratory campaign aimed at measuring the missing production and destruction cross sections is envisaged for a large number of nuclei, isotopes, anti-nuclei and positrons, in the perspective of a reliable interpretation of the direct measurements on galactic cosmic rays.

### *7.7.3 Dark Matter searches*

Dark Matter (DM) in the form of Weakly Interactive Massive Particles (WIMPs) can be detected observing the particles produced in the annihilation (or in some models in the decay) of the DM particles forming the invisible halo of our galaxy. The charged particles produced in the annihilations or decay remain partially confined by the galactic magnetic field and can be observed as an excess over the expected fluxes generated by known mechanisms. The best sensitivity is obtained measuring the flux of anti–particles such as positrons and anti–protons, which have a smaller background from known processes. The dominant known source of anti–protons in cosmic radiation is due to the interactions of cosmic rays with the interstellar medium gas (in reactions such as $pp \rightarrow ppp\bar{p} + X$). Uncertainty in the production of anti–nucleons in $pp$ and $p\mathrm{He}$ interactions in the interesting energy range $E \lesssim M$ (with $M \sim$ 10–1000 GeV the mass of the DM particles) can be as large as 50% at the highest energies. This energy range is accessible with accelerator experiments. The interest of these studies is discussed in [913].

### *7.7.4 Atmospheric neutrinos*

Another field of research where a program of measurements of hadronic interaction properties could reduce systematic errors is the study of neutrino oscillations using atmospheric neutrinos. New large mass Cherenkov neutrino telescopes (PINGU [916] and ORCA [917]) have been proposed with the main goal to determine the neutrino mass hierarchy (normal or inverted) from a precision measurement of the energy and zenith angle distributions of atmospheric neutrinos. Extensions of this program could also be sensitive to the phase $\delta$ in the PMNS neutrino mixing matrix. Precision measurements of proton interactions on an air target would allow a more precise prediction of the no-oscillation flux.